

# Observation of localization using a noisy quantum computer

Kazue Kudo<sup>1,2,\*</sup>

<sup>1</sup>*Department of Computer Science, Ochanomizu University, Tokyo 112-8610, Japan*

<sup>2</sup>*Graduate School of Information Sciences, Tohoku University, Sendai 980-8579, Japan*

(Dated: March 23, 2023)

Quantum dynamics in a strongly-disordered quantum many-body system show localization properties. The initial state memory is maintained due to slow relaxation when the system is in the localized regime. This work demonstrates how localization can be probed in a noisy quantum computer by evaluating the magnetization and twist overlap in a quantum spin chain after a short-time evolution. Those quantities obtained from the exact time evolution and quantum-circuit simulation show apparent dependence on the disorder strength. Similar behavior is observed in real-device computation, indicating that short-time quantum dynamics can distinguish between thermal and localized behavior.

## I. INTRODUCTION

Localization in quantum systems has been investigated in a wide variety of contexts. Many-body localization (MBL) is eigenstate localization in strongly-disordered interacting systems and can be regarded as an extended concept of Anderson localization. Although MBL has been investigated for decades, it still attracts great attention [1–4]. Many numerical studies have demonstrated features of a continuous transition from the thermal to localized phases by investigating quantities evaluated using eigenstates [5–17] and quantum dynamics [18–20]. However, exponents of the finite-size scaling analysis in quenched disordered systems violate the Harris criterion [21, 22], which indicates that the system sizes in those numerical studies are too small to analyze the MBL transition. In other words, the transition observed in the numerical works of finite-size systems is not a true phase transition but a crossover. Although the existence of the true MBL phase is controversial, the MBL transition point is located at a much stronger disorder if it exists [23–26]. In this work, when a finite-size system shows some MBL properties, we say that the system is in the localized regime.

Typical methods to detect MBL in experiments are based on the memory effect. Because of slow relaxation in the localized regime, the initial state remains almost the same for a long time. Experimental works often investigate simple quantities, such as imbalance and magnetization, which are easily obtained from the measurement of qubits [27–36]. However, it is difficult to extract information on eigenstates from imbalance or magnetization. In contrast, twist overlap, which is also easily obtained from qubit measurements, shows characteristic behavior beyond the memory effect and can reflect the information on eigenstates [37]: The twist overlap based on quantum dynamics behaves similarly to the one evaluated using eigenstates.

This work examines whether localization can be de-

tected using a gate-model quantum computer, inspired by experiments of localization detection using a quantum annealer [36]. The quantum annealer has difficulty making a significant difference between interaction and local fields. By contrast, in a gate-model quantum device, parameters for interaction and local fields are independent, and thus one can control the disorder strength separately. Focusing on the disorder dependence of the magnetization and twist overlap, we compare the results of numerical simulations and those of a small noisy quantum computer. The simulation of time evolution using a gate-model quantum computer suffers from approximation error due to Suzuki-Trotter decomposition [38, 39]. A large Trotter number reduces the approximation error but increases the number of quantum gates, which causes gate errors. Thus, the balance between the approximation and gate errors is critical in a noisy quantum device.

The purpose of this paper is to demonstrate how localization can be probed in a noisy quantum computer beyond the memory effect. To reduce the effect of noise, we focus on a short-time behavior instead of long-time evolution. Quantum-circuit simulations show the same behavior as the exact time evolution. The twist overlap suffers more than magnetization from errors. Real-device computation in this work indicate that short-time quantum dynamics can distinguish thermal and localized behavior in a small-size system.

## II. MODEL AND METHODS

The Hamiltonian of a one-dimensional transverse Ising model with local random fields consists of the Ising Hamiltonian  $H_I$  and the transverse-field Hamiltonian  $H_{TF}$ :  $H = H_I + H_{TF}$ , where

$$H_I = \sum_{j=1}^{L-1} J \sigma_j^z \sigma_{j+1}^z + \sum_{j=1}^L h_j \sigma_j^z, \quad (1)$$

$$H_{TF} = - \sum_{j=1}^L \Gamma \sigma_j^x. \quad (2)$$

\* kudo@is.ocha.ac.jp

Here,  $L$  is the system size, and  $\sigma_j^x$  and  $\sigma_j^z$  are the Pauli operators of components  $x$  and  $z$ , respectively, at site  $j$ . The interaction is antiferromagnetic, and thus  $J$  is positive. The strength of the transverse field  $\gamma$  is also taken as positive. These parameters are fixed as  $J = \Gamma = 1$  in the following. The local fields  $h_j$  are given as uniformly distributed random numbers in the interval  $[-w, w]$ , where  $w$  denotes the disorder strength.

We observe the magnetization and twist overlap at the end of the time evolution, namely, at the final time  $t = T_{\text{fin}}$ . Both observables are easily obtained in a quantum device by measuring each qubit. Those observables averaged over different disorder realizations are useful for probing localization [37]. The initial state is given as the all-spin-up state in this study.

The magnetization  $M_z = \langle \psi | \sum_j \sigma_j^z | \psi \rangle$ , where  $|\psi\rangle$  is a wavefunction, in the  $z$  direction is initially equal to the system size  $L$ . The magnetization relaxes to zero because of antiferromagnetic interactions in a weak-disorder case. In contrast, the magnetization is expected to keep the initial value due to the memory effect when the disorder is strong.

The twist overlap  $z = \langle \psi | U_{\text{twist}} | \psi \rangle$  is the overlap between a state  $|\psi\rangle$  and its twisted state  $U_{\text{twist}}|\psi\rangle$ . Here,  $U_{\text{twist}}$  is the twist operator defined by

$$U_{\text{twist}} = \exp \left[ i \sum_{j=1}^L \theta_j \sigma_j^z / 2 \right]. \quad (3)$$

The twist operator generates a spin-wave-like excitation by rotating the spins around the  $z$  axis at angles  $\theta_j = 2\pi j/L$  [40, 41]. When  $|\psi\rangle$  is a thermal eigenstate, the twist overlap vanishes because the twisted state with a spin-wave-like excitation is orthogonal to the original state. However, the long-wavelength perturbation given by the twist operator has little effect on localized eigenstates, which leads to a finite twist overlap. The twist overlap can be evaluated using a wavefunction that is a linear combination of eigenstates. The disorder dependence of the twist overlap evaluated with eigenstates behaves similarly to the one evaluated with wavefunctions after time evolution [37].

Time evolution is based on the Schrödinger equation,

$$i \frac{d}{dt} |\psi(t)\rangle = H |\psi(t)\rangle, \quad (4)$$

whose solution is represented as

$$|\psi(t)\rangle = e^{-iHt} |\psi_0\rangle, \quad (5)$$

where  $|\psi_0\rangle$  denotes the initial state. The wavefunction  $|\psi(t)\rangle$  at any time can be obtained from the exact diagonalization of the Hamiltonian. Writing the initial state as a linear combination  $|\psi_0\rangle = \sum_k c_k |\phi_k\rangle$  of the eigenstates  $|\phi_k\rangle$  yields

$$|\psi(t)\rangle = \sum_{k=1}^{2^L} c_k e^{-iE_k t} |\phi_k\rangle, \quad (6)$$

where  $E_k$  is the eigenenergy corresponding to  $|\phi_k\rangle$ . We here refer to the time dependence of wavefunctions obtained from the exact diagonalization as the exact time evolution.

For quantum simulations using quantum circuits, one needs to approximate the time evolution operator using product formulas [38, 39]. Using the first-order Suzuki-Trotter decomposition, we have

$$e^{-iH\tau} = e^{-i(H_1+H_{T1})\tau} = \left( e^{-iH_1\delta} e^{-iH_{T1}\delta} \right)^m, \quad (7)$$

where  $\delta = \tau/m$  and  $m$  is called the Trotter number or Trotter steps. Similarly, the second-order Suzuki-Trotter decomposition leads to

$$e^{-iH\tau} = \left( e^{-iH_{T1}\delta/2} e^{-iH_1\delta} e^{-iH_{T1}\delta/2} \right)^m. \quad (8)$$

The Trotter error of the  $p$ th-order decomposition is in the order of  $O(\delta^{p+1})$ . Unitary operators  $e^{-i(\theta/2)\sigma_j^x}$  and  $e^{-i(\theta/2)\sigma_j^z}$  are implemented by single-qubit rotation gates,  $R_j^X(\theta)$  and  $R_j^Z(\theta)$ , applied to the  $j$ th qubit, respectively. Similarly, operators of interaction terms are implemented by two-qubit  $ZZ$  rotation gates.

For computation on a real quantum computer, we use `ibmq_manila`, which is one of the IBM Quantum Falcon Processors. It is a five-qubit quantum computer and has a linear structure. The simple execution of quantum circuits introduced above suffers from errors in real noisy quantum hardware. We use noise mitigation techniques to reduce errors without fault tolerance strategies [42].

We compare quantum-circuit simulations and real-device computation with the result based on the exact time evolution. In the simulations and real-device computation, observables are evaluated by measurements with 1024 shots per circuit.

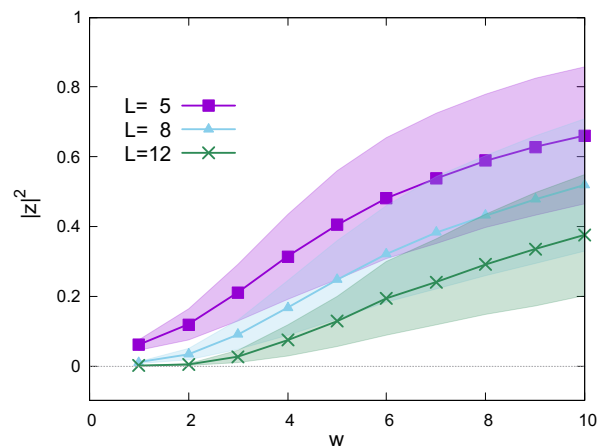


FIG. 1. Disorder dependence of the twist overlap  $|z|^2$  evaluated with eigenstates for different system sizes. The error bars represent the standard deviation.

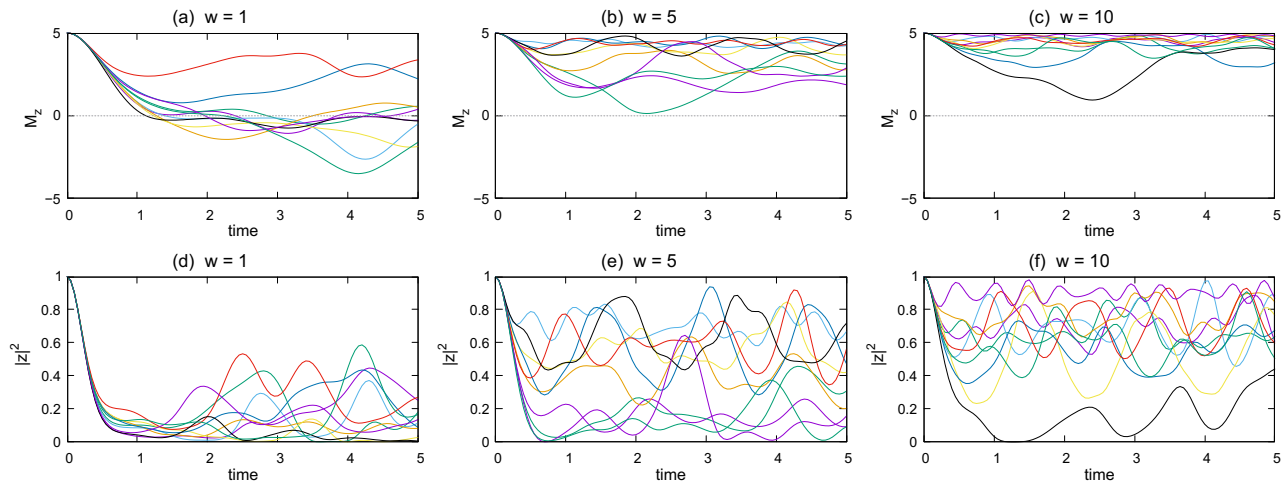


FIG. 2. Time dependence of (a–c) the magnetization in the  $z$  direction  $M_z$  and (d–f) the absolute square of the twist overlap  $|z|^2$  for  $L = 5$ . Ten different samples are plotted in each panel. (a) and (d) share the same samples of wavefunctions, and the same applies to (b) and (e), and (c) and (f).

### III. RESULTS

First, we examine the twist overlap  $z$  evaluated with eigenstates to compare with those evaluated with wavefunctions after time evolution. Figure 1 shows the disorder-strength dependence of the absolute square of the twist overlap  $|z|^2$  averaged over different disorder realizations. The number of realizations is  $10^4$  for  $L = 5, 8$ , and  $10^3$  for  $L = 12$ . The twist overlap is calculated and averaged over 16 (for  $L = 5$ ) or 20 eigenstates (for  $L = 8, 12$ ) around the center of the energy spectrum. Since the crossover from the thermal to localized regimes is expected to occur around  $w \sim 1-5$  [37], we here focus on the region from  $w = 1$  to  $w = 10$ . Even for a small system such as  $L = 5$ , the twist overlap behaves the same as shown in Ref. [37]: While  $z$  is significantly small for a small  $w$ , the average and variance of  $|z|^2$  grow as  $w$  increases.

Next, we determine the final time  $T_{\text{fin}}$  of time evolution to evaluate the magnetization and twist overlap. Figure 2 illustrates the time evolution of the magnetization in the  $z$  direction  $M_z$  and the absolute square of twist overlap  $|z|^2$  for ten different disorder realization samples. They are calculated from the exact time evolution for  $L = 5$ . For a weak disorder case ( $w = 1$ ), the initial decay of  $M_z$  ceases around  $t \simeq 1$ , and that of  $|z|^2$  does before  $t = 1$ . These results indicate that the final time should be  $T_{\text{fin}} > 1$ . To reduce errors due to noise, a short  $T_{\text{fin}}$  is preferable. Thus, we take  $T_{\text{fin}} = 1.5$ , which is long enough, especially for middle or strong disorder cases.

Figure 3 demonstrates results of quantum-circuit simulations computed using a classical computer. Simulation results with a label  $(p, m)$  are calculated using the  $p$ th-order Suzuki-Trotter decomposition with Trotter number  $m$ . The system size is  $L = 5$ , and data are averaged over  $10^4$  disorder realization samples. The results la-

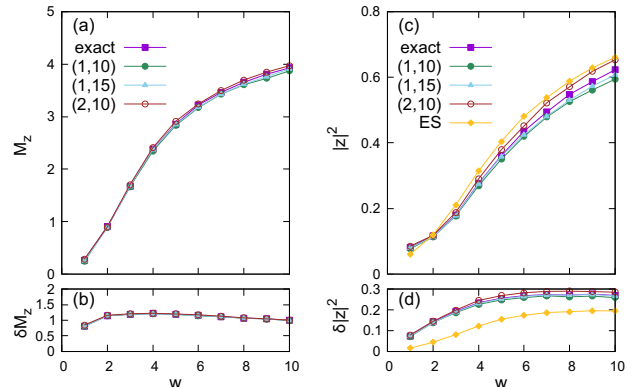


FIG. 3. Disorder dependence of (a,b) the magnetization in the  $z$  direction  $M_z$  and (c,d) the absolute square of the twist overlap  $|z|^2$ . Plots labeled exact are calculated using the exact time evolution. Plots with label  $(p, m)$  are simulation results for the  $p$ th-order Suzuki-Trotter decomposition with Trotter number  $m$ . Data labeled ES are the same as Fig. 1 ( $L = 5$ ). Panels (a) and (c) plot the average, and panels (b) and (d) plot the standard deviation.

beled exact are obtained from the exact time evolution. The disorder dependence of  $M_z$  for simulations is almost identical to that for the exact time evolution.

Simulation results of the twist overlap are compared with the result based on the exact time evolution and the one evaluated with eigenstates (labeled ES). The plots with the label ES are the same as Fig. 1 ( $L = 5$ ). The average of  $|z|^2$  shows similar behavior to the result based on the exact time evolution and the one obtained from eigenstates. In contrast, the standard deviation  $\delta|z|^2$  for the result obtained from eigenstates is smaller than the others. Simulation results using the first-order Suzuki-Trotter decomposition are smaller than the exact-time-

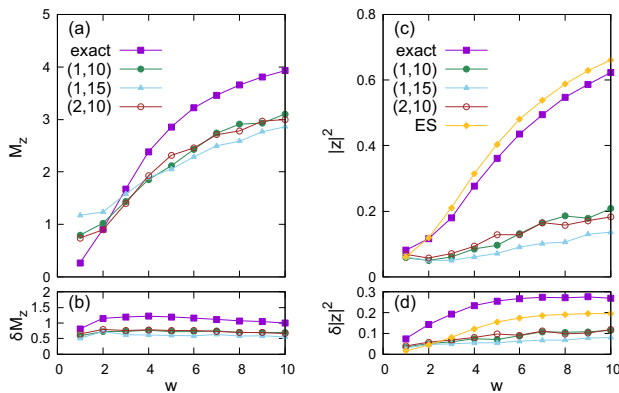


FIG. 4. Disorder dependence of (a,b) the magnetization in the  $z$  direction  $M_z$  and (c,d) the absolute square of the twist overlap  $|z|^2$ . Plots with label  $(p,m)$  are real-device results for the  $p$ th-order Suzuki-Trotter decomposition with Trotter number  $m$ . Plots labeled exact and ES are the same as those in Fig. 3. Panels (a) and (c) plot the average, and panels (b) and (d) plot the standard deviation.

evolution result, while the result using the second-order one is larger than the exact result.

Real-device results shown in Fig. 4 indicate that errors due to noise are significant. Data labeled  $(p,m)$  are calculated using the  $p$ th-order Suzuki-Trotter decomposition with Trotter number  $m$  and averaged over  $10^3$  disorder realization samples. The disorder dependence of magnetization  $M_z$  using a real device has an increasing behavior. However, the average of  $M_z$  is smaller than the result based on the exact time evolution, especially in a large- $w$  region. The average and standard deviation of  $|z|^2$  obtained from real-device computation increase with the disorder strength, although they are much smaller than those based on the exact time evolution.  $M_z$  and  $|z|^2$  suffer from more significant errors for  $m = 15$  than for  $m = 10$ , while the difference between  $p = 1$  and  $p = 2$  is negligible.

#### IV. DISCUSSION AND CONCLUSIONS

Figure 4(a) illustrates that the averaged  $M_z$  shows an evident dependence on the disorder strength  $w$ , even though results suffer from errors. As shown in Fig. 2, the memory effect, which comes from slow dynamics and indicates localization, is evident in a large- $w$  region. Large

values of  $M_z$  in Fig. 4(a) reflect the memory effect. The result suggests that the memory effect is robust against noises, which is also supported in other real-device experiments [36].

Compared with the magnetization, the twist overlap is vulnerable to noises, as shown in Figs. 4(c) and (d). The vulnerability suggests that the memory effect on the twist overlap is weak. The time dependence of  $|z|^2$  that is shown in Figs. 2(d)–(g) demonstrates that the memory effect does not work on some samples. The previous work [37] suggested that the twist overlap can provide information on eigenstates beyond the memory effect. However, errors due to noises cause difficulty in obtaining information on eigenstates. Nevertheless, real-device computation in a more extensive system would provide a clearer  $w$  dependence of the twist overlap because the twist overlap is expected to vanish in a small- $w$  region for a large system, as shown in Fig. 1

In this work, Trotter numbers are chosen so that the Trotter errors in quantum-circuit simulations are acceptable for evaluating the magnetization and twist overlap. The larger the Trotter number, the better the approximation accuracy. However, errors due to noises become significant in real-device computation as the Trotter number increases. The number of two-qubit gates, whose errors are much more significant than that of a single-qubit gate, is proportional to the Trotter number and is the same in the first and second-order Suzuki-Trotter decomposition. Thus, errors are more affected by the Trotter number than by the order of the Suzuki-Trotter decomposition.

In conclusion, quantum simulations using a real noisy device can detect the crossover between thermal and localized regimes. The magnetization and twist overlap evaluated after time evolution increase with the disorder strength on average, although the rise is weaker in real-device results than in simulator results. These results suggest some hints to probe localization using a real quantum computer.

#### ACKNOWLEDGMENTS

We acknowledge the use of IBM Quantum services for this work. The views expressed are those of the author, and do not reflect the official policy or position of IBM or the IBM Quantum team.

[1] S. A. Parameswaran and R. Vasseur, Many-body localization, symmetry and topology, Rep. Prog. Phys. **81**, 082501 (2018).  
 [2] D. A. Abanin, E. Altman, I. Bloch, and M. Serbyn, Colloquium: Many-body localization, thermalization, and entanglement, Rev. Mod. Phys. **91**, 021001 (2019).

[3] S. Gopalakrishnan and S. A. Parameswaran, Dynamics and transport at the threshold of many-body localization, Phys. Rep. **862**, 1 (2020).  
 [4] K. S. Tikhonov and A. D. Mirlin, From Anderson localization on random regular graphs to many-body localization, Ann. Phys. Special Issue on Localisation 2020, **435**,

- 168525 (2021).
- [5] A. Pal and D. A. Huse, Many-body localization phase transition, *Phys. Rev. B* **82**, 174411 (2010).
- [6] M. Serbyn, Z. Papić, and D. A. Abanin, Local Conservation Laws and the Structure of the Many-Body Localized States, *Phys. Rev. Lett.* **111**, 127201 (2013).
- [7] M. Serbyn and J. E. Moore, Spectral statistics across the many-body localization transition, *Phys. Rev. B* **93**, 041424(R) (2016).
- [8] V. Khemani, F. Pollmann, and S. L. Sondhi, Obtaining Highly Excited Eigenstates of Many-Body Localized Hamiltonians by the Density Matrix Renormalization Group Approach, *Phys. Rev. Lett.* **116**, 247204 (2016).
- [9] V. Khemani, S. P. Lim, D. N. Sheng, and D. A. Huse, Critical Properties of the Many-Body Localization Transition, *Phys. Rev. X* **7**, 021013 (2017).
- [10] V. Khemani, D. N. Sheng, and D. A. Huse, Two Universality Classes for the Many-Body Localization Transition, *Phys. Rev. Lett.* **119**, 075702 (2017).
- [11] S. Bera, H. Schomerus, F. Heidrich-Meisner, and J. H. Bardarson, Many-Body Localization Characterized from a One-Particle Perspective, *Phys. Rev. Lett.* **115**, 046603 (2015).
- [12] S. Bera and A. Lakshminarayan, Local entanglement structure across a many-body localization transition, *Phys. Rev. B* **93**, 134204 (2016).
- [13] J. A. Kjäll, J. H. Bardarson, and F. Pollmann, Many-Body Localization in a Disordered Quantum Ising Chain, *Phys. Rev. Lett.* **113**, 107204 (2014).
- [14] D. J. Luitz, N. Laflorencie, and F. Alet, Many-body localization edge in the random-field Heisenberg chain, *Phys. Rev. B* **91**, 081103(R) (2015).
- [15] M. Hopjan and F. Heidrich-Meisner, Many-body localization from a one-particle perspective in the disordered one-dimensional bose-hubbard model, *Phys. Rev. A* **101**, 063617 (2020).
- [16] J. Gray, S. Bose, and A. Bayat, Many-body localization transition: Schmidt gap, entanglement length, and scaling, *Phys. Rev. B* **97**, 201105(R) (2018).
- [17] K. Kudo and T. Deguchi, Finite-size scaling with respect to interaction and disorder strength at the many-body localization transition, *Phys. Rev. B* **97**, 220201(R) (2018).
- [18] J. H. Bardarson, F. Pollmann, and J. E. Moore, Unbounded Growth of Entanglement in Models of Many-Body Localization, *Phys. Rev. Lett.* **109**, 017202 (2012).
- [19] M. Serbyn, Z. Papić, and D. A. Abanin, Universal Slow Growth of Entanglement in Interacting Strongly Disordered Systems, *Phys. Rev. Lett.* **110**, 260601 (2013).
- [20] T. Enss, F. Andraschko, and J. Sirker, Many-body localization in infinite chains, *Phys. Rev. B* **95**, 045121 (2017).
- [21] A. B. Harris, Effect of random defects on the critical behaviour of ising models, *J. Phys. C: Solid State Phys.* **7**, 1671 (1974).
- [22] J. T. Chayes, L. Chayes, D. S. Fisher, and T. Spencer, Finite-size scaling and correlation lengths for disordered systems, *Phys. Rev. Lett.* **57**, 2999 (1986).
- [23] J. Z. Imbrie, On Many-Body Localization for Quantum Spin Chains, *J. Stat. Phys.* **163**, 998 (2016).
- [24] P. Sierant and J. Zakrzewski, Challenges to observation of many-body localization, *Phys. Rev. B* **105**, 224203 (2022).
- [25] A. Morningstar, L. Colmenarez, V. Khemani, D. J. Luitz, and D. A. Huse, Avalanches and many-body resonances in many-body localized systems, *Phys. Rev. B* **105**, 174205 (2022).
- [26] D. Sels, Bath-induced delocalization in interacting disordered spin chains, *Phys. Rev. B* **106**, L020202 (2022).
- [27] M. Schreiber, S. S. Hodgman, P. Bordia, H. P. Lüschen, M. H. Fischer, R. Vosk, E. Altman, U. Schneider, and I. Bloch, Observation of many-body localization of interacting fermions in a quasirandom optical lattice, *Science* **349**, 842 (2015).
- [28] J. Smith, A. Lee, P. Richerme, B. Neyenhuis, P. W. Hess, P. Hauke, M. Heyl, D. A. Huse, and C. Monroe, Many-body localization in a quantum simulator with programmable random disorder, *Nat. Phys.* **12**, 907 (2016).
- [29] P. Bordia, H. P. Lüschen, S. S. Hodgman, M. Schreiber, I. Bloch, and U. Schneider, Coupling identical one-dimensional many-body localized systems, *Phys. Rev. Lett.* **116**, 140401 (2016).
- [30] P. Bordia, H. Lüschen, S. Scherg, S. Gopalakrishnan, M. Knap, U. Schneider, and I. Bloch, Probing Slow Relaxation and Many-Body Localization in Two-Dimensional Quasiperiodic Systems, *Phys. Rev. X* **7**, 041047 (2017).
- [31] H. P. Lüschen, P. Bordia, S. S. Hodgman, M. Schreiber, S. Sarkar, A. J. Daley, M. H. Fischer, E. Altman, I. Bloch, and U. Schneider, Signatures of Many-Body Localization in a Controlled Open Quantum System, *Phys. Rev. X* **7**, 011034 (2017).
- [32] H. P. Lüschen, P. Bordia, S. Scherg, F. Alet, E. Altman, U. Schneider, and I. Bloch, Observation of Slow Dynamics near the Many-Body Localization Transition in One-Dimensional Quasiperiodic Systems, *Phys. Rev. Lett.* **119**, 260401 (2017).
- [33] K. Xu, J.-J. Chen, Y. Zeng, Y.-R. Zhang, C. Song, W. Liu, Q. Guo, P. Zhang, D. Xu, H. Deng, K. Huang, H. Wang, X. Zhu, D. Zheng, and H. Fan, Emulating Many-Body Localization with a Superconducting Quantum Processor, *Phys. Rev. Lett.* **120**, 050507 (2018).
- [34] T. Kohlert, S. Scherg, X. Li, H. P. Lüschen, S. Das Sarma, I. Bloch, and M. Aidelsburger, Observation of Many-Body Localization in a One-Dimensional System with a Single-Particle Mobility Edge, *Phys. Rev. Lett.* **122**, 170403 (2019).
- [35] A. Rubio-Abadal, J.-y. Choi, J. Zeiher, S. Hollerith, J. Rui, I. Bloch, and C. Gross, Many-Body Delocalization in the Presence of a Quantum Bath, *Phys. Rev. X* **9**, 041014 (2019).
- [36] J. L. C. da C. Filho, Z. G. Izquierdo, A. Saguia, T. Albash, I. Hen, and M. S. Sarandy, Localization transition induced by programmable disorder, *Phys. Rev. B* **105**, 134201 (2022).
- [37] K. Kudo, Localization Detection Based on Quantum Dynamics, *Entropy* **24**, 1085 (2022).
- [38] N. Hatano and M. Suzuki, Finding Exponential Product Formulas of Higher Orders, in *Quantum Annealing and Other Optimization Methods*, Lecture Notes in Physics, edited by A. Das and B. K. Chakrabarti (Springer, Berlin, Heidelberg, 2005) pp. 37–68.
- [39] A. M. Childs, Y. Su, M. C. Tran, N. Wiebe, and S. Zhu, Theory of trotter error with commutator scaling, *Phys. Rev. X* **11**, 011020 (2021).
- [40] M. Nakamura and S. Todo, Order Parameter to Characterize Valence-Bond-Solid States in Quantum Spin Chains, *Phys. Rev. Lett.* **89**, 077204 (2002).
- [41] T. Kutsuzawa and S. Todo, Nested Iterative Shift-invert Diagonalization for Many-body Localiza-

tion in the Random-field Heisenberg Chain, e-print arXiv:2203.09732 (2022).

[42] K. J. Ferris, A. Rasmuson, N. T. Bronn, and O. Lanes,

Quantum simulation on noisy superconducting quantum computers, arXiv preprint arXiv:2209.02795 (2022).